Statistical analysis of high-frequency multibeam backscatter data in shallow water

P.J.W. Siwabessy, A.N. Gavrilov, A.J. Duncan and I.M. Parnum

Centre for Marine Science and Technology, Curtin University of Technology, Perth, Australia

ABSTRACT

The seabed type of most shallow water areas is very often not homogenous but patchy in space and changeable with time. Recent studies have shown that statistics of acoustic backscatter from an inhomogeneous seabed deviate significantly from a conventional Rayleigh model and may show distributions with multiple modes and heavier tails. In this work, seabed backscatter statistics are analysed using the data collected with a RESON SeaBat 8125 multibeam sonar system (operating at 455kHz) in the regions of Recherche Archipelago and Cockburn Sound in Western Australia. The 455-kHz acoustic backscatter data were collected over areas consisting of different seabed types, including sand, rhodolith, seagrass and bedrock. Statistical models of backscatter intensity from these different seabed types were investigated for different values of the incident angle. The goodness of fit for the model with the experimental distributions was assessed with the nonparametric Kolmogorov-Smirnoff (KS) test statistic. Before compensation for the angular dependence of backscatter, the Rayleigh mixture probability distribution function provides the best fit to all experimental distributions at *near-nadir* angles of incidence. Within *moderate* and *oblique* angle intervals, the log-normal distribution fits experimental distributions best around the centre of the distributions and the Rayleigh 3-component mixture distribution in most cases provides the best fits to the tail of the distributions. After the angular correction, the log-normal distribution fits empirical distributions best in all cases, but the Rayleigh mixture distribution offers the best fits to the tail of distributions for seagrass and bedrock seafloors.

INTRODUCTION

Multibeam sonar systems have rapidly advanced over the last few decades, and are currently the most efficient acoustic remote sensing tools for seabed mapping, as they offer a rapid assessment of both bathymetry and acoustic backscatter properties of the seabed over a wide coverage area. Modern high-resolution multibeam sonar systems form hundreds of narrow receive beams (about 1^{o} wide) and transmit short pulses of several tens of microseconds at high frequencies (hundreds of kHz). Hence, they are capable of resolving small features in the seafloor relief.

Most shallow water seabeds are not homogeneous as often assumed in statistical analysis of acoustic backscatter but are patchy in space and changeable in time. Backscatter from seagrass covered seabeds, for example, may be varying in time because of the motion of seagrass due to swells or currents, which causes temporal changes in the number and configuration of individual scattering objects within the insonified area on the seabed. For narrow-beam sonar systems and a shallow water environment, the insonified area and the footprints of receive beams on the seafloor are small so that the number of statistically independent individual scatterers, contributing simultaneously to the backscattered sound field, is not sufficient to approximately satisfy the central limit theorem. Consequently, backscatter statistics do not conform to the conventional Rayleigh model valid for the magnitude of normally distributed complex processes.

Recent studies have noted a non-Rayleigh character of backscatter statistics for shallow water seabeds and suggested different models, such as Rayleigh mixture distribution and *K*-distribution models (Gallaudet and de Moustier 2003; Hellequin *et al*. 2003; Lyons and Abraham 1999; Abraham 1997; Dunlop 1997; Stewart *et al.* 1994; Jakeman 1988), and log-normal distribution models (Trevorrow 2004; Stanic and Kennedy 1992; Gensane 1989). While Stanic and Kennedy (1992) preferred the log-normal distribution models for large incidence angles, Lyons and Abraham (1999) favoured Rayleigh mixture distribution and *K*-distribution models for all angles of incidence. Gallaudet and de Moustier (2003), and Lyons and Abraham (1999) also found that the backscatter statistics exhibited statistical distributions with heavier tails and multiple modes.

This paper presents results of a statistical analysis of 455-kHz acoustic backscatter data collected with a RESON SeaBat 8125 multibeam sonar system in shallow water. While in many studies of backscatter statistics, measurements were conducted from fixed platforms, data used in this study were obtained from real multibeam surveys aboard moving vessels, and hence they incorporated fluctuations of the backscatter strength due to the influence of spatial variability. Areas of distinctly different seabed habitat types such as sand, rhodolith (a calcareous algae), seagrass and bedrock were selected from the data collected in two different trips in the Recherche Archipelago and Cockburn Sound areas in Western Australia.

EXPERIMENTAL DATA AND DATA ANALYSIS

Table 1. Specifications of RESON SeaBat 8125 sonar

Operating Frequency	455 kHz
Swath Coverage	120º (3.5×water depth)
Beam Width, Along Track	1.0º
Beam Width, Across Track	0.5º (at nadir)
Number of Horizontal Beams	240
Range Resolution	1.0 cm
Maximum Ping Rate	40 pings per second

The principal characteristics of the SeaBat 8125 sonar system are given in Table 1. The Recherche Archipelago study site selected for analysis was 15 m to 45 m deep with sand, rhodolith, and bedrock on the seabed. The seabed area selected in Cockburn Sound was covered with seagrass and the water depth varied from 8 m to 16 m. The acoustic backscatter images of the study sites before and after angular compensation are shown in Figure 1. For the time when these two surveys were conducted, the SeaBat 8125 sonar system had not yet been calibrated, and therefore the backscatter strength values in Figure 1 are shown in dBs relative to a common reference value. Grab samples were collected over the surveyed areas to verify the bottom type. Terrain analysis of the bathymetry data was used to identify areas of bedrock.

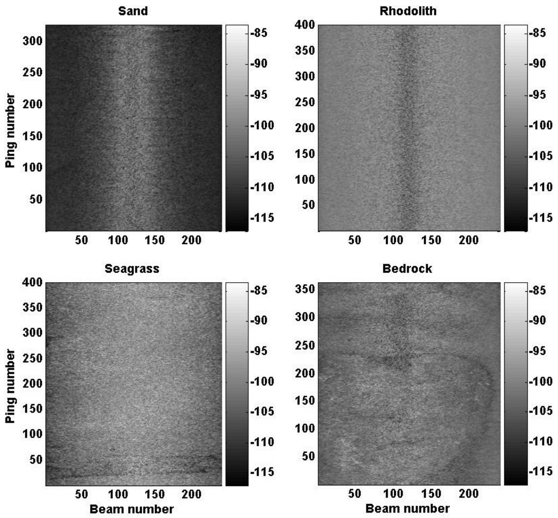

(a) Before angular compensation

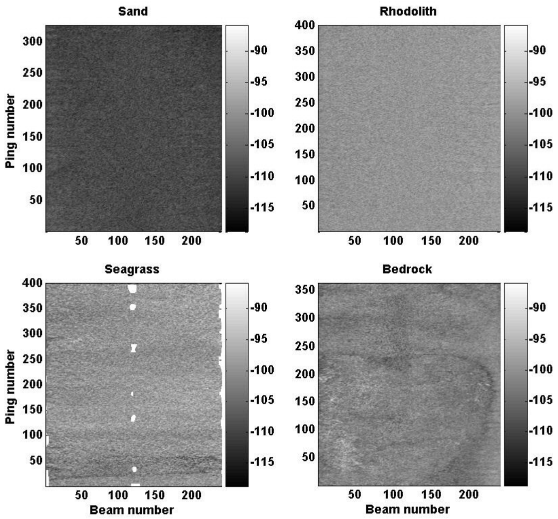

(b) After angular compensation

Figure 1. Acoustic backscatter images for the four selected sites of different seabed habitat types.

Backscattering strength

Previous attempts made at correcting the angular dependence of seabed backscatter through theoretical models seem to be inadequate, especially for the high frequency multibeam systems such as the SeaBat 8125. The simplest Lambert's model, used frequently for compensating backscatter values for the angular dependence, is not suitable for the 455-kHz carrier frequency of the SeaBat 8125 system used here. At such a high frequency, the Rayleigh parameter, i.e. the product of the surface roughness height and the vertical wavenumber, becomes much greater than unity. This makes the small perturbation approximation inappropriate for modelling backscatter at any incidence angle. There are no universal backscattering models suitable for every seabed type at high frequencies. An empirical approach based on removing the spatially averaged angular response derived for a single swath track or its sections of certain length (Gavrilov *et al.* 2005a; Beaudoin *et al.* 2002) is an alternative method for angular correction, which was employed in this study. The procedure of building an equalised backscatter image of the seabed independent of system settings, environmental conditions and incidence angles, as outlined in Gavrilov *et al.* (2005b) and Parnum *et al.* (2006), involves six steps which are as follows:

1. Calculate the true angles of incidence corrected for the ship motion and for the local slope of the seabed surface;
2. Remove time varying gain correction applied to the intensity of backscatter signals by the system hardware;
3. Correct the backscatter intensity data for the system settings, including transmit power, gain and pulse length;
4. Calculate the backscatter coefficients from backscatter intensity data corrected for the spreading and absorption losses using the actual distance to the seabed and an estimate of the acoustic absorption coefficient. The pulse-average backscatter intensity is also corrected for the beam footprint size;
5. Derive the mean angular dependence of backscatter from the backscatter coefficients and the true angles of incidence;
6. Compensate the backscatter coefficients for the mean angular dependence and restore the absolute backscatter level using the reference value of mean backscatter intensity at moderate angles of 30 - 31^{o}.

A modified algorithm used in this study for the angular compensation of backscatter also involved correction for the angular dependence of backscatter intensity variance. Details of the modified algorithm are given in Parnum *et al.* (2006).

Probability distribution models

The statistical distribution models used in this study are the Rayleigh, *K*, Rayleigh mixture and log-normal distributions. These models are commonly used to approximate the statistical distribution of acoustic backscatter data. Some of them are associated with the physical scattering mechanisms. The *K* and Rayleigh mixture distributions have the Rayleigh distribution as a submember.

The probability density functions (PDFs) and their associated cumulative distribution functions (CDFs) of the distribution models used in this study are presented in Table 2. The Rayleigh distribution results when the number of statistically independent, randomly distributed scatterers within the insonified area, is large enough for the central limit theorem to hold. Stanton (1984; 1985) has shown that the Rayleigh distribution is a special case of the Ricean distribution that applies when incoherent scattering is dominant. The *K*-distribution, first used to describe the statistics of sea surface clutter in radar data by Jakeman and Pusey (1976), is a product of a rapidly fluctuating Rayleigh distributed component and a slowly varying chi-distributed component (Ward 1981). The Rayleigh mixture distribution model is a multimodal Rayleigh distribution occurring as a result of a superposition of a number of Rayleigh scattering processes originating from different types of scattering material mixed in the seabed cover, and hence having their own contribution to the resulting backscatter intensity. This distribution model is of particular importance in an inhomogeneous, shallow water environment in which acoustic backscattering is driven by several independent scattering mechanisms. Whereas all other distribution models used in this analysis may be related to certain physical scattering mechanisms through their association with the Rayleigh model, the log-normal distribution model has not yet been analytically related to any physical scattering processes. Many studies of underwater acoustic backscatter, however, have observed the log-normal distribution of backscatter data (e.g. Trevorrow 2004; Stanic and

Kennedy 1992; Chotiros *et al.* 1985). Trevorrow (2004) observed a variation of backscatter distributions between the log-normal and Rayleigh distribution models whereas Stanic and Kennedy (1992) observed high-frequency shallow-water backscatter variations obeying the Gaussian distribution model at small incidence angles and the log-normal distribution at large incidence angles. Chotiros *et al.* (1985) showed that high-frequency seafloor backscattering could depart from a Rayleigh distribution depending on the beamwidth. The wide-beam seafloor backscattering followed the Rayleigh distribution whereas the narrow-beam seafloor backscattering obeyed the log-normal distribution.

Table 2. Distribution functions.

Distribution	Type	Expression
Log-normal	PDF	$\frac{\alpha}{\sqrt{2\pi}x} e^{-\frac{(\beta+\alpha\log x)^2}{2}}$
	CDF	$\Phi(\beta+\alpha\log x)$
Rayleigh	PDF	$\frac{2x}{\lambda} e^{-\frac{x^2}{\lambda}}$
	CDF	$1-e^{-\frac{x^2}{\lambda}}$
Rayleigh mix.	PDF	$\sum_{i=1}^{m}\varepsilon_i \frac{2x}{\lambda_i} e^{-\frac{x^2}{\lambda_i}}$
	CDF	$1-\sum_{i=1}^{m}\varepsilon_i e^{-\frac{x^2}{\lambda_i}}$
K	PDF	$\frac{4}{\sqrt{\alpha}\Gamma(\nu)}\left(\frac{x}{\sqrt{\alpha}}\right)^{\nu} K_{\nu-1}\left(\frac{2x}{\sqrt{\alpha}}\right)$
	CDF	$1-\frac{1}{\Gamma(\nu)2^{\nu-1}}\left(\frac{2x}{\sqrt{\alpha}}\right)^{\nu} K_{\nu}\left(\frac{2x}{\sqrt{\alpha}}\right)$

Statistical analysis

Four selected distribution models were fitted to the experimental distribution of backscatter data. This required the CDF parameters of the candidate distribution models to be estimated. A maximum likelihood method and a method of moments were used for the analysis. In the maximum likelihood method, parameters of the candidate distribution models are estimated to maximise the likelihood function. In the method of moments, the model parameters are selected to equate the first few moments of the distribution model and the experimental distribution, as described in Abraham (1997) and implemented in Abraham (1997), Lyons and Abraham (1999), and Gallaudet and de Moustier (2003). Both experimental and theoretical distributions are presented in all plots in this study as the probability of false alarm (PFA=1-CDF) to emphasise the tail portion of the distributions, which is of particular importance for multimodal or heavier tail distributions.

A nonparametric Kolmogorov-Smirnoff (KS) statistical test was used to assess the goodness of fit between the theoretical and experimental distributions. It defines the maximum absolute difference (D_{KS}) between the theoretical and experimental CDFs. The *p*-value of D_{KS}, that indicates the probability of observing an absolute difference greater than D_{KS} under the null hypothesis (H_o), was utilised for a comparison of the goodness of fit. The *p*-value tends to unity as the absolute difference between the theoretical and experimental CDFs tends to zero. The KS test results were accepted with caution because the theory of the KS test is not satisfied when the CDF parameters of model distributions are derived from experimental data (Lyons and Abraham 1999). However, this test provides a satisfactory measure of the goodness of fit between the model and experimental CDFs. In addition to the *p*-value, the root mean square difference (D_{rms}) between the model and experimental CDFs, as outlined in Gallaudet and de Moustier (2003), was used in this analysis as a relative measure of the goodness of fit of the two CDFs. The root mean square difference (d_{rms}) derived only from the samples in the distributions where PFA < 10^{-2} and called *tail rms difference* in Gallaudet and de Moustier (2003) was also used in the analysis to highlight multimodal/heavier tail distributions which are likely to exist in the groups which are characterised by large kurtosis shown in Table 3.

Table 3. Summary of groups of data for statistical analysis: 1=*near-nadir* (-10° to 10°); 2=*moderate* (20° to 40°); 3=*oblique* (>40°): c denotes group of data after angular compensation.

Group	Type	Depth, m	Mean BS, dB	Kurtosis
S1		43.9-44.2	-102.82	3.9523
S1c			-109.34	0.5032
S2		43.9-44.2	-108.88	4.9484
S2c	Sand		-109.07	1.6035
S3		43.9-44.4	-110.81	0.7778
S3c			-108.72	2.4428
R1		41.7-42.4	-101.92	3.0888
R1c			-99.59	0.0582
R2		41.4-42.1	-99.88	6.6824
R2c	Rhodolith		-99.85	2.5736
R3		40.8-42.0	-100.87	1.1114
R3c			-100.21	1.4095
SG1		9.0-9.6	-97.90	18.68
SG1c			-100.07	39.98
SG2		9.0-9.7	-100.33	14.91
SG2c	Seagrass		-100.29	15.77
SG3		8.8-9.8	-104.39	28.15
SG3c			-100.64	42.08
BR1		22.8-34.8	-101.53	13.0524
BR1c			-102.37	4.5138
BR2		19.9-32.0	-101.68	18.1467
BR2c	Bedrock		-101.71	18.6028
BR3		16.5-29.5	-103.46	20.3569
BR3c			-102.11	51.5011

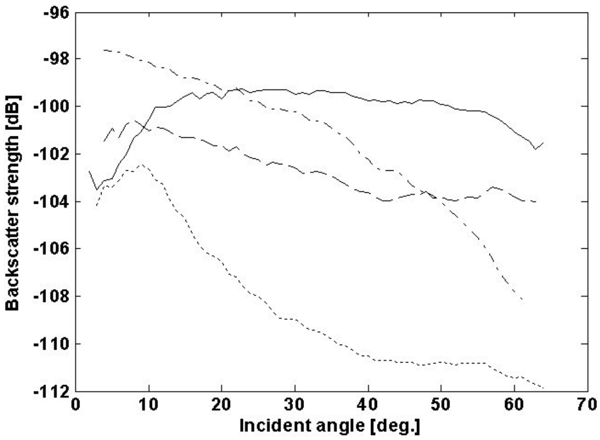

Figure 2. Mean angular response curve of different seabed habitat types: – Rhodolith; … Sand; – – Bedrock; and –.– Seagrass.

Data preparation

It seems impractical to perform a statistical analysis for every incidence angle across the track for each data set of different seabed habitat type. Grouping data by a few different angular domains within each data set is reasonable because the backscatter statistical characteristics are expected to change slowly with the incidence angle. The angular dependence of the mean backscatter level shown in Figure 2 for all four seabed types investigated in this study was used to determine different characteristic domains of the incident angle. Three angular domains were finally adopted for all data sets: 1) *near-nadir* (-10° to 10°), 2) *moderate* (20° to 40°) and 3) *oblique* (>40°). A summary of all backscatter data used for the statistical analysis is given in Table 3 grouped by the seabed types observed within different angular domains.

RESULTS AND DISCUSSIONS

The *p*-values for sand and rhodolith from this study compare well with those for coarse sand, sand/shell and seagrass *posidonia* given in Lyons and Abraham (1999) and for the so-called "seafloor backscatter" presented in Gallaudet and de Moustier (2003). Results of the statistical analysis are summarised in Tables 4 and 5. Table 4 lists all distribution models having the *p*-value for D_{KS} above the significance level (α) of 0.05 with the highest one shown in bold. The highest *p*-values shown as bold in Table 4 also associate in all cases with the lowest D_{rms} values. Table 5 shows distribution models having the lowest d_{rms} value. Results shown in Table 5 do not always match those shown in Table 4, indicating the presence of the heavier tail and multiple mode distributions.

The log-normal distribution is present in almost all cases, but do not always have the highest *p*-value. Of twenty-three log-normal distributions observed, only nine have a *p*-value greater than 0.7.

Before angular compensation at *near-nadir* angles in all seabed groups, the Rayleigh (3-component) mixture distribution fits the experimental distribution best, as seen in Figure 3, with the typical *p*-values greater than 0.9. A closer investigation of the estimated parameters of the Rayleigh mixture model reveals that in most cases only two components are dominating in the model as was also found by Lyons and Abraham (1999). Although the *K*-distribution also fits the experimental distribution quite well, the *p*-value for the *K*-distribution model is lower than that of the Rayleigh mixture model. At *moderate* and *oblique* angles, however (see Figures 4 and 5), the log-normal distribution provides the best fit to the experimental distributions for all groups in terms of the *p*-value. This suggests that the experimental distribution for all groups tends to the log-normal distribution as the incidence angle increases. While the *p*-value for the log-normal distribution is increasing with the incidence angle, the *p*-value for the Rayleigh mixture distribution is generally decreasing. In addition to the log-normal distribution, the Rayleigh mixture distribution is also a good approximation to the experimental distribution of the seagrass backscatter data in the *moderate* and *oblique* angle regimes, shown respectively in Figures 4(c) and 5(c), with reasonably high *p*-values (>0.5).

Based on the d_{rms} value (Table 5), the Rayleigh mixture distribution provides the best fit to the tail of the experimental distributions in the *moderate* angle regime for all seabed groups except the rhodolith cover. This suggests that the rhodolith cover was flatter than the others while sand in the investigated area might be slightly undulated as indicated by a slightly heavier tail in Figure 4(a) opposed to a normal tail in Figure 4(b) for rhodolith. The undulation, however, is small since neither d_{rms} value nor *p*-value supports the Rayleigh mixture distribution for sand in the *oblique* angle regime as shown in Figure 5(a).

Although the log-normal distribution provides the best fit to the experimental distributions for seagrass and bedrock at the *moderate* and *oblique* angles of incidence in terms of the *p*-value, much heavier tails are observed in the experimental data as indicated by lower d_{rms} values. Examples of heavier tails at *moderate* and *oblique* angles are shown in Figures 4(c) and 5(c) for seagrass and in 4(d) and 5(d) for bedrock.

Table 4. CDF model tendency based on *p*-value of D_{KS} as a function of incidence angles and seabed habitat types. Model with highest *p*-value is shown in bold.

Seabed type	Incidence angle domain		
	Near-nadir	*Moderate*	*Oblique*
(a) Before angular compensation			
Sand	LN, **RM**, K	**LN**	**LN**
Rhodolith	LN, **RM**, K	LN	LN
Seagrass	**RM**	**LN**, RM	**LN**, RM
Bedrock	LN, **RM**	LN	LN
(b) After angular compensation			
Sand	LN	**LN**	**LN**
Rhodolith	**LN**	LN	LN
Seagrass	LN, **RM**	**LN**, RM	**LN**, RM
Bedrock	**LN**	LN	**LN**

Table 5. CDF tail model tendency based on d_{rms} as a function of incidence angles and seabed habitat types.

Seabed type	Incidence angle domain		
	Near-nadir	*Moderate*	*Oblique*
(a) Before angular compensation			
Sand	RM	RM	LN
Rhodolith	RM	**LN**	**LN**
Seagrass	RM	RM	LN
Bedrock	K	**RM**	**RM**
(b) After angular compensation			
Sand	**R, RM**	R, RM	LN
Rhodolith	R, RM	**R, RM**	**LN**
Seagrass	K	LN	K
Bedrock	RM	**RM**	RM

The multimodal distribution with heaver tails suggests that the seagrass and bedrock areas were essentially inhomogeneous due to spatial patchiness of the seagrass and bedrock roughness.

After angular compensation, the log-normal distribution model, in most cases, matches the experimental distributions better than any others in terms of the *p*-value. Results for the *near-nadir*, *moderate* and *oblique* angle regimes are presented in Figures 6, 7 and 8 respectively. In general, a slight increase in the *p*-value of the log-normal distribution appeared after angular compensation. For the sand and rhodilith seabeds, which are both fairly flat, the Rayleigh mixture distribution model coincides with the Rayleigh distribution model in all angular regimes. This suggests that only one component is strongly dominating in the Rayleigh mixture distribution model and the other components have been suppressed, most likely as a result of angular compensation. In contrast to sand and rhodolith, no match between the Rayleigh model and the Rayleigh mixture model can be observed in the seagrass and bedrock data in every angular domain. A heavier tail still exists after angular compensation in the seagrass and bedrock backscatter distributions and in the *moderate* and *oblique* incidence angle regimes. The most likely reason for this is a higher large-scale roughness and more contrast in spatial patchiness of the bedrock and seagrass roughness, the influence of which cannot be reduced by angular correction. A smaller *p*-value of the Rayleigh mixture model is observed for bedrock and seagrass.

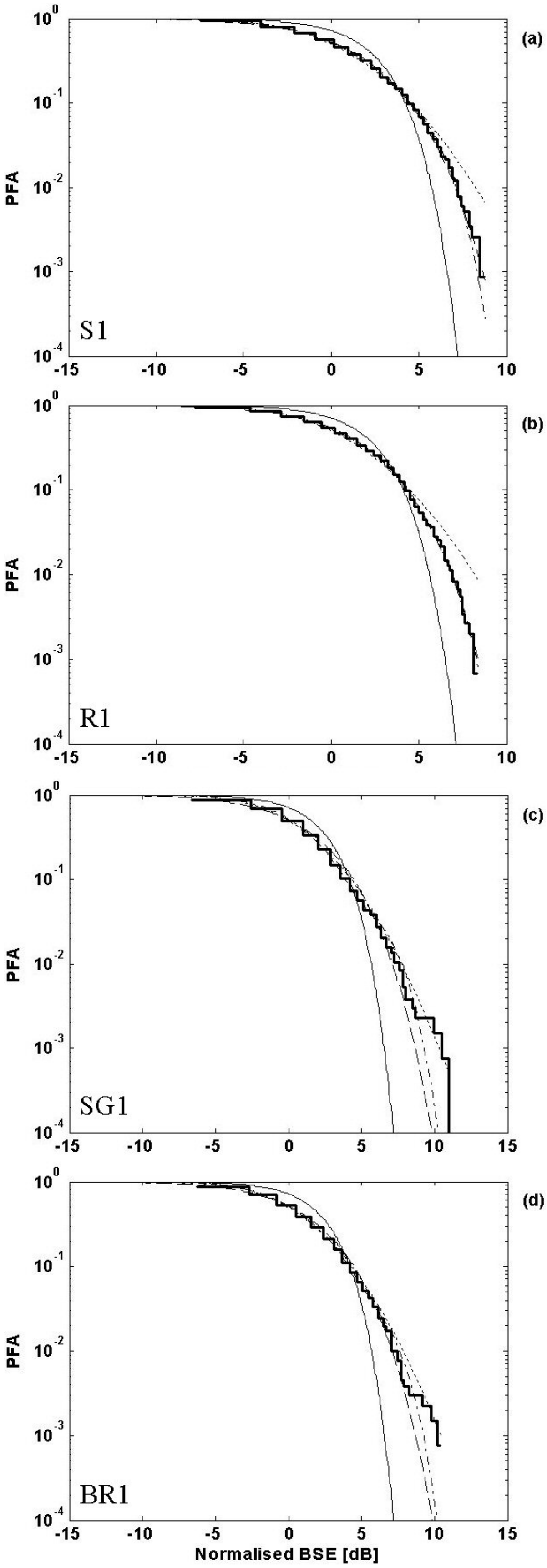

Figure 3. Probability of false alarm for sand, rhodolith, seagrass and bedrock seafloors (a, b, c and d respectively) at the *near-nadir* angle regime (-10^o to 10^o) before angular compensation. –Rayleigh, …Log-normal, – –*K* and –.–Rayleigh mixture.

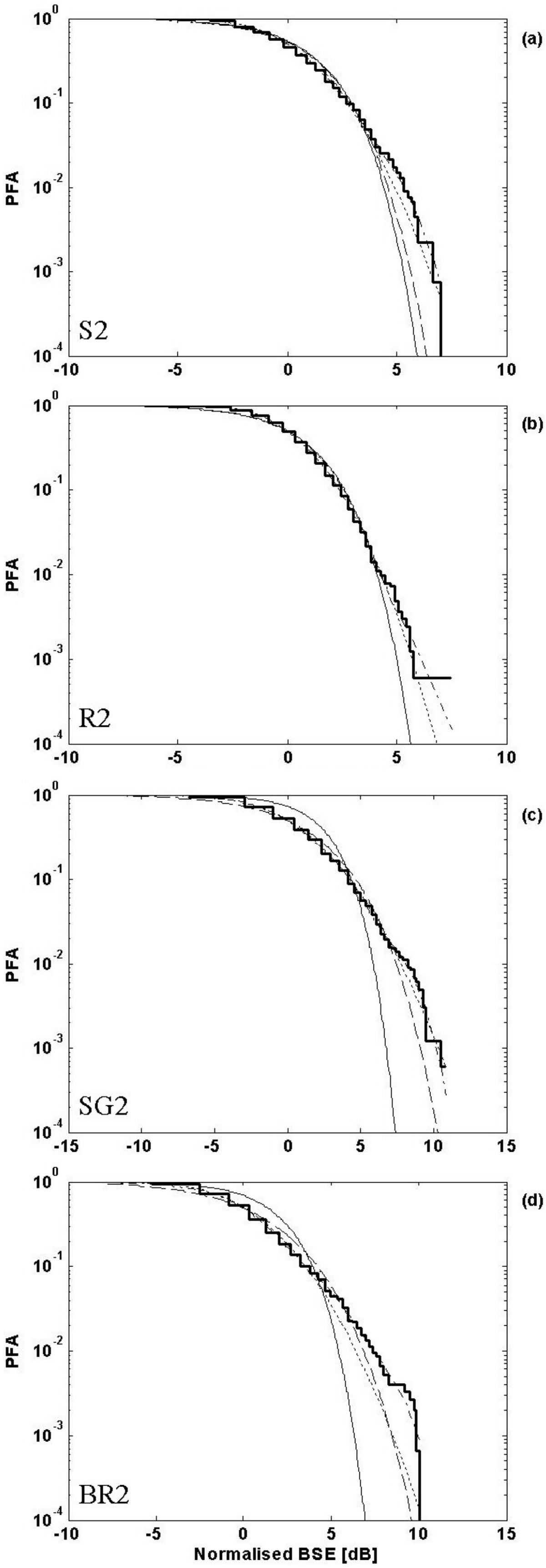

Figure 4. Probability of false alarm for sand, rhodolith, seagrass and bedrock seafloors (a, b, c and d respectively) at the *moderate* angle regime (20^o to 40^o) before angular compensation. –Rayleigh, …Log-normal, – –*K* and –.–Rayleigh mixture.

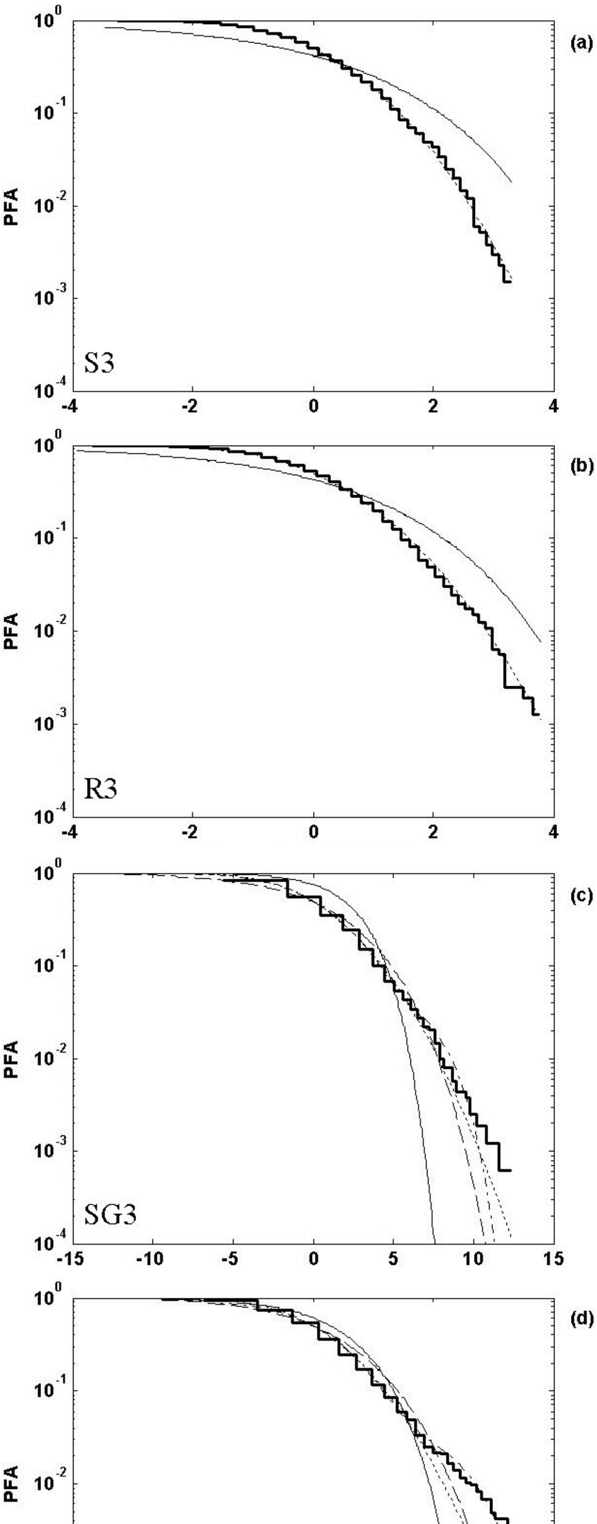

Figure 5. Probability of false alarm for sand, rhodolith, seagrass and bedrock seafloors (a, b, c and d respectively) at the *oblique* angle regime (>40^o) before angular compensation. –Rayleigh, …Log-normal, – –*K* and –.–Rayleigh mixture.

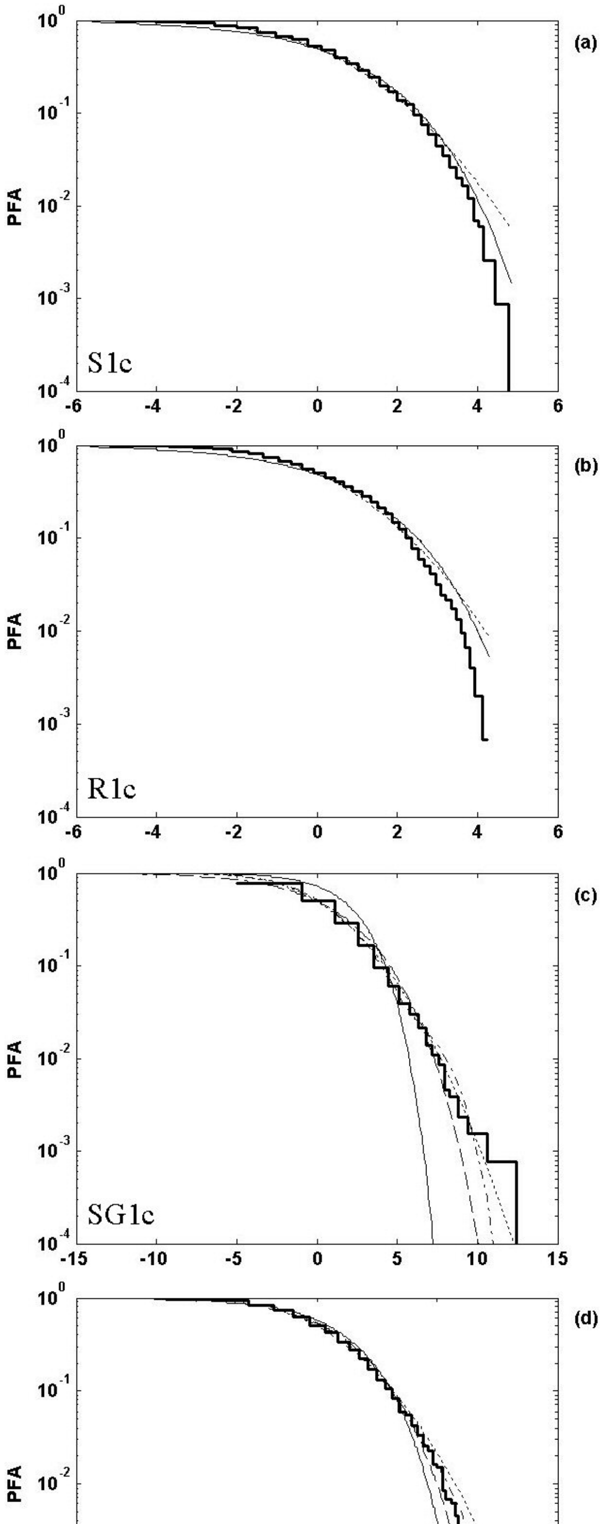

Figure 6. Probability of false alarm for sand, rhodolith, seagrass and bedrock seafloors (a, b, c and d respectively) at the *near-nadir* angle regime (-10^o to 10^o) after angular compensation. –Rayleigh, …Log-normal, – –*K* and –.–Rayleigh mixture.

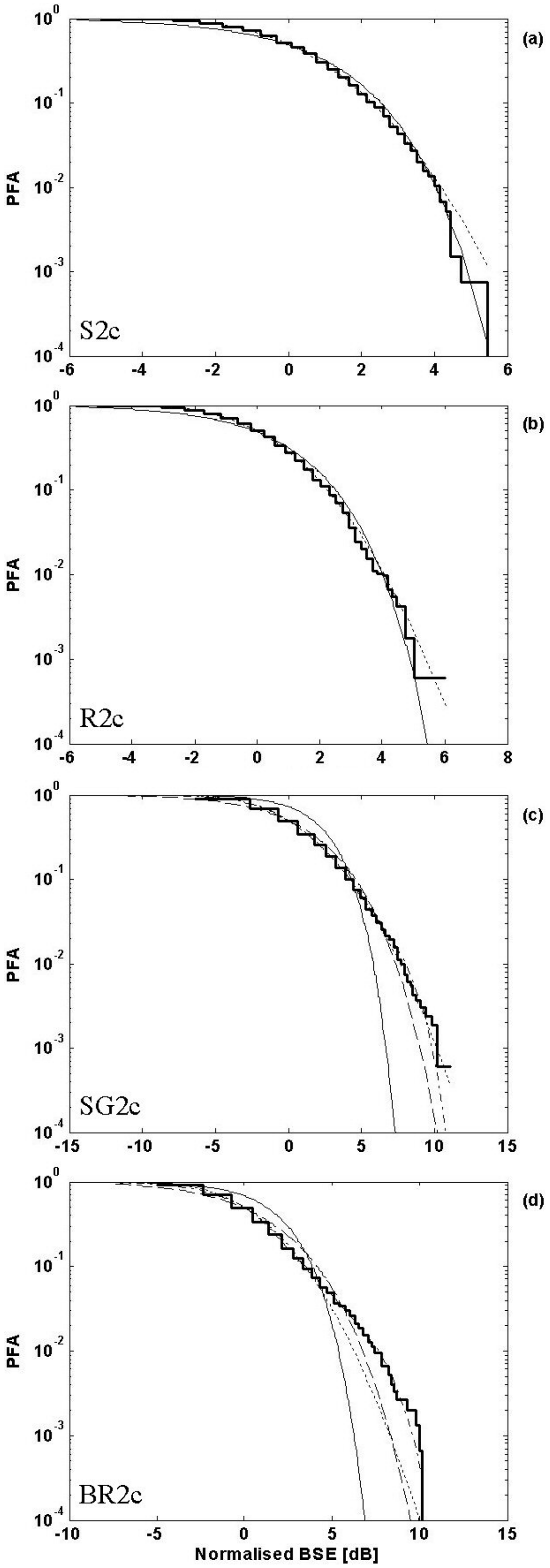

Figure 7. Probability of false alarm for sand, rhodolith, seagrass and bedrock seafloors (a, b, c and d respectively) at the *moderate* angle regime (20^o to 40^o) after angular compensation. –Rayleigh, …Log-normal, – –*K* and –.–Rayleigh mixture.

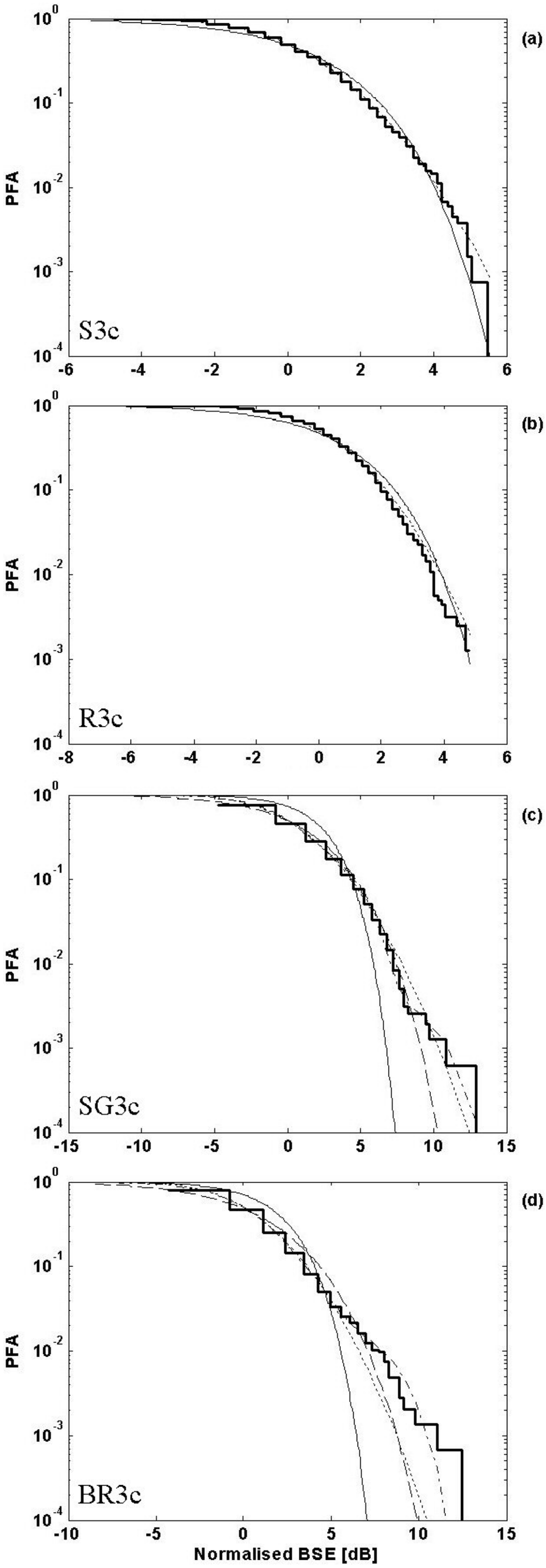

Figure 8. Probability of false alarm for sand, rhodolith, seagrass and bedrock seafloors (a, b, c and d respectively) at the *oblique* angle regime (>40^o) after angular compensation. –Rayleigh, …Log-normal, – –*K* and –.–Rayleigh mixture.

CONCLUSIONS

The statistical distribution of seafloor backscatter strength was investigated for four different seabed types using the data from two different multibeam surveys conducted in shallow water.

Non-Rayleigh distributions have been observed in all cases. Either a Rayleigh mixture or log-normal distributional model best fits the backscatter data depending on the incidence angle and seafloor type in terms of its homogeneity and roughness scale.

The experimental distributions for all groups of habitats tend towards the log-normal distribution as the incidence angle increases. In addition, the experimental distribution for sand and rhodolith approaches the log-normal as the angle of incidence increases faster than that for seagrass and bedrock. For a complex seabed type such as seagrass and bedrock, multi-scale roughness components are present. This leads to an incoherent superposition of the Rayleigh distribution with different parameters at different incidence angles insonified at different times and thereby originates a multimodal Rayleigh distribution (Rayleigh mixture). The experimental distribution of the seafloor backscattering will therefore depend upon the scale of roughness relative to the insonified area and the angle of incidence.

The log-normal distribution model has been observed either alone or together with other distribution models in all cases in this study. The empirical angular compensation developed by Parnum *et al.* (2006) seems to suppress some components, small-scale roughness in particular, contributing to the Rayleigh mixture distribution and retains components contributing to the log-normal distribution. This is indicated by an increase in the *p*-values of the Rayleigh and log-normal distributions and a decrease in the *p*-values of the Rayleigh mixture distribution after angular compensation.

Results of this study have shown that the Kolmogorov-Smirnoff statistic test tends to describe the fit to the bodies of the distributions only but not the fit to the tails. The Anderson-Darling statistic test (Stephens 1974), a modified Kolmogorov-Smirnoff test, is being considered for future analysis.

ACKNOWLEDGEMENTS

The authors would like to thank the Coastal Water Habitat Mapping (CWHM) project within the Cooperative Research Centre for Coastal Zone, Estuary and Waterway Management (Coastal CRC) for their continued support and funding.

REFERENCES

Abraham, D.A. 1997, *Modelling non-Rayleigh reverberation*, SACLANT Undersea Research Center Report SR-266.

Beaudoin, J., Hughes Clarke, J., van den Ameele, E., and Gardner, J. 2002, "Geometric and radiometric correction of multibeam backscatter derived from Reson 8101 systems." *Proceedings of the Canadian Hydrographic Conference* 2002, Canadian Hydrographic Association, Ottawa, Ontario, Summer, CD-ROM, pp. 8.

Chotiros, N.P., Boehme, H., Goldsberry, T.G., Pitt, S.P., Lamb, R.A., Garcia, A.L., and Altenburg, R.A. 1985, "Acoustic backscatter at low grazing angles from the ocean bottom. Part II. Statistical characteristics of bottom backscatter at a shallow water site." *Journal of the Acoustical Society of America* 77(3): 975-982.

Dunlop, J. 1997, "Statistical modelling of sidescan sonar images." *Proc. MTS/IEEE Oceans '97 Conf.* v.1, pp. 33-38.

Gallaudet, T.C., and de Moustier, C.P. 2003, "High-frequency volume and boundary acoustic backscatter fluctuations in shallow water." *Journal of the Acoustical Society of America* 114(2): 707-725.

Gavrilov, A.N, Duncan, A.J., McCauley, R.D., Parnum, I. M., Penrose, J. D., Siwabessy, P. J. W., Woods, A. J., and Tseng, Y-T. 2005a, "Characterization of the seafloor in Australia's coastal zone using acoustic techniques." *Proceedings of Underwater Acoustic Measurements Conference*, Heraklion, Crete, Greece, June 2005.

Gavrilov, A.N., Siwabessy, P.J.W., and Parnum, I.M. 2005b, "Multibeam echo sounder backscatter analysis: Theory review, methods and application to Sydney Harbour swath data." CRC Milestone Report CA3.03, CMST Report 2005-03 for the Cooperative Research Centre for Coastal Zone, Estuary and Waterway Management. Centre for Marine Science and Technology, Curtin University of Technology, Perth, Australia.

Gensane, M. 1989, "A statistical study of acoustic signals backscattered from the sea bottom." *IEEE Journal of Oceanic Engineering* 14(1): 84-93.

Hellequin, L., Boucher, J.M., and Lurton, X. 2003, "Processing of high-frequency multibeam echo sounder data for seafloor characterization." *IEEE Journal of Oceanic Engineering* 28(1): 78-89.

Jakeman, E. 1988, "Non-Gaussian models for the statistics of the scattered waves", *Advances in Physics* 37(5): 471-529.

Jakeman, E., and Pusey, P.N. 1976, "A model for non-Rayleigh sea echo." *IEEE Transactions on Antennas and Propagation* 24(6): 806-814.

Lyons, A.P., and Abraham D.A. 1999, "Statistical characterization of high-frequency shallow-water seafloor backscatter." *Journal of the Acoustical Society of America* 106(3): 1307-1315.

Parnum, I.M., Gavrilov, A.N., Siwabessy, P.J.W., and Duncan, A.J. 2006, "Analysis of high-frequency multibeam backscatter statistics from different seafloor habitats." *Proceedings of the Eight European Conference on Underwater Acoustics*, Carvoeiro, Portugal, June 2006. p775-780.

Stanic, S., and Kennedy, E. 1992, "Fluctuations of high-frequency shallow water seafloor reverberation." *Journal of the Acoustical Society of America* 91(4): 1967-1973.

Stanton, T.K. 1985, "Echo fluctuations from the rough seafloor: Predictions based on acoustically measured microrelief properties." *Journal of the Acoustical Society of America* 78(2): 715-721.

Stanton, T.K. 1984, "Sonar estimates of seafloor microroughness." *Journal of the Acoustical Society of America* 75(3): 809-818.

Stephens, M.A. 1974, "EDF statistics for goodness of fit and some comparisons." *Journal of the American Statistical Association* 69(347): 730-737.

Stewart, W.K., Chu, D., and Malik, S. 1994, "Quantitative seafloor characterization using a bathymetric sidescan sonar." *IEEE Journal of Oceanic Engineering* 19(4): 599-610.

Trevorrow, M.V. 2004, "Statistics of fluctuations in high-frequency low-grazing-angle backscatter from a rocky sea bed." *IEEE Journal of Oceanic Engineering* 29(2): 236-245.

Ward, K.D. 1981, "Compound representation of high resolution sea clutter." *Electronics Letters* 17: 561-563.